

UCSF

UC San Francisco Previously Published Works

Title

Chronic multisite brain recordings from a totally implantable bidirectional neural interface: experience in 5 patients with Parkinson's disease.

Permalink

<https://escholarship.org/uc/item/2vw761xw>

Journal

Journal of neurosurgery, 128(2)

ISSN

0022-3085

Authors

Swann, Nicole C
de Hemptinne, Coralie
Miocinovic, Svjetlana
[et al.](#)

Publication Date

2018-02-01

DOI

10.3171/2016.11.jns161162

Peer reviewed



Published in final edited form as:

J Neurosurg. 2018 February ; 128(2): 605–616. doi:10.3171/2016.11.JNS161162.

Chronic multisite brain recordings from a totally implantable bidirectional neural interface: experience in five patients with Parkinson's disease

Nicole C Swann, PhD¹, Coralie de Hemptinne, PhD¹, Svjetlana Miocinovic, MD, PhD², Salman Qasim, BS¹, Jill L Ostrem, MD², Nicholas B Galifianakis, MD², Marta San Luciano, MD², Sarah S Wang, PhD², Nathan Ziman, BS², Robin Taylor, MSN, FNP², and Philip A Starr, MD, PhD^{1,3,4}

¹Department of Neurological Surgery, University of California, San Francisco, CA 94143

²Department of Neurology, University of California, San Francisco, CA 94143

³Kavli Institute for Fundamental Neuroscience

⁴University of California, San Francisco Graduate Program in Neuroscience

Abstract

OBJECTIVE—Dysfunction of distributed neural networks underlies many brain disorders. Development of neuromodulation therapies depends on a better understanding of these networks. Invasive human brain recordings have a favorable temporal and spatial resolution for the analysis of network phenomena, but have generally been limited to acute intraoperative recording or short term recording through temporarily externalized leads. Here we describe our initial experience with an investigational, totally implantable, first generation, bidirectional neural interface that allows for both continuous therapeutic stimulation and recordings of field potentials at multiple sites in a neural network.

METHODS—We implanted five Parkinson's disease patients with Activa PC+S (*Medtronic Inc.*), under a physician-sponsored Food and Drug Administration investigational device exemption. The device was attached to a quadripolar lead placed in the subdural space over motor cortex, for recording of electrocorticography (ECoG) potentials, and to a quadripolar lead in subthalamic nucleus (STN) for both therapeutic stimulation and recording of local field potentials (LFPs). We recorded from each patient at multiple time points over a one year period.

RESULTS—There were no serious surgical complications or interruptions of DBS therapy. Signals in both cortex and STN were relatively stable over time, despite a gradual increase in electrode impedance. We were able to identify canonical movement related changes in specific frequency bands in motor cortex in most but not all recordings.

*Please address correspondence to: Dr. Nicole C. Swann, 513 Parnassus HSE 8, Room 823, San Francisco, CA 94143, Phone: 415-514-2154, Fax: 415-353-3907, Nicole.Swann@ucsf.edu.

Disclosures: Implanted devices and technical support were provided at no charge by *Medtronic Inc.* under a research agreement. Medtronic engineers also reviewed the manuscript for technical accuracy. University of California, San Francisco has filed a preliminary patent application based on results using Activa PC+S. NCS, CDH, JLO, and PAS are co-inventors on this patent.

CONCLUSION—Acquisition of chronic multisite field potentials in humans is feasible. Device performance characteristics described here may inform the design of the next generation of totally implantable neural interfaces. This research tool provides a platform for translation of discoveries in brain network dynamics to improved neurostimulation paradigms.

Keywords

Deep Brain Stimulation (DBS); Parkinson’s disease (PD); brain machine interface (BMI); basal ganglia; motor cortex; electrophysiology

Introduction

Much has been learned about brain networks in Parkinson’s disease (PD) from invasive brain recordings in patients undergoing neurosurgery in the awake state. Signals studied intraoperatively include basal ganglia single unit discharge³⁹, basal ganglia local field potentials (LFPs)²², and motor cortex electrocorticography (ECoG) potentials²³. LFPs and ECoG potentials mainly reflect summed, synchronized synaptic activity from neuronal populations close to the recording electrode. LFPs have also been studied through temporarily externalized basal ganglia deep brain stimulation (DBS) leads, allowing recording for several days postoperatively¹³. Together, these recording approaches have redefined PD as a circuit disorder characterized by excessive neuronal synchronization²², led to a mechanistic understanding of the effects of acute DBS¹¹, and suggested strategies to improve DBS therapy by incorporating feedback control¹⁴.

However, intraoperative and short term perioperative recordings from externalized leads suffer from several disadvantages: severe time and logistical restrictions, the confounding influence of the “microlesion” effect, in which brain circuits are perturbed by edema around recently inserted leads¹⁶, increased infection risk (in the case of externalized leads)³, and the inability to assess chronic effects of therapies or to prototype strategies for chronic closed-loop control (automated adjustment of DBS stimulation parameters based on brain signals).

To address these shortcomings, we launched an investigational protocol utilizing a first generation, totally implantable, “bidirectional neural interface”, a prosthesis that both delivers clinically indicated stimulation therapy and senses and stores brain activity. This device, Activa PC+S (*Medtronic, Inc*), allows chronic, intermittent collection of field potential data over years, initiated either by investigators in the clinic, by patients in their homes, or by automated algorithms^{1,2,30,32,33}. The device is available to research groups worldwide under investigator-initiated protocols, or under CE Mark in European countries^{15,20,27}. In our study, the stimulation/sensing pulse generator is attached to both a basal ganglia and a cortical electrode array, to allow multisite recordings for network-level analyses. Here, we report our initial experience with the device in five PD patients over one year, focusing on the implantation technique, complications, recording capabilities, technical limitations that should guide future device development, and solutions for researchers to mitigate these limitations with the current device.

Methods

Patients

Inclusion criteria for this study were: a diagnosis of idiopathic PD by a movement disorders neurologist and clinical justification for DBS surgery based on the presence of motor fluctuations or medication-induced dyskinesia after treatment with anti-parkinsonian medications at maximal tolerable levels. Patients with prominent tremor were excluded, since tremor is not present in all patients and physiology related to tremor may be distinct^{8,26}.

Patients provided written consent in agreement with the declaration of Helsinki and the University of California, San Francisco (UCSF) institutional review board (protocol # 13-108). The study also was reviewed and approved by the Food and Drug Administration (FDA) under a physician sponsored investigational device exemption (IDE # G120283). The study was registered at Clinical Trials.gov (NCT01934296).

Activa PC+S recording capabilities

Functional capabilities of PC+S have been detailed in preclinical publications^{1,2,30,32,33}. Briefly, the device has 8-channel connectivity, but voltage time series may be recorded from only two bipolar channels simultaneously. Available sampling rates are 200, 422, and 800 Hz. Intrinsic filters applied to the time series channels depend on the sampling rate. For 800 Hz (the sampling rate we used most often) there was a 0.5 Hz high pass filter (1 pole, RC), a 260 Hz anti-aliasing filter (3 pole, RC filter), and a 1000 Hz low pass filter (1 pole, RC). There was also the option of increasing the high pass filter to 8 Hz (1 pole, RC) and decreasing the low pass filter to 100 Hz (1 pole, RC). Two additional channels may be selected for simultaneous calculation and storage of spectral power in pre-specified bandwidths, but we did not systematically test that capability. When sampling two time series channels continuously at the maximum sampling rate of 800 Hz, the maximum recording duration that can be stored, before data downloading to an external computer is required, is 8 minutes and 42 seconds. Data compression algorithms can increase the length of recordings that can be stored, but we did not systematically use these algorithms as our early experience suggested that they decreased the signal-to-noise ratio. The Activa PC+S is identical in shape and size to the standard FDA-approved Activa PC device commonly used for therapeutic neurostimulation in movement disorders.

Surgery

The subthalamic nuclei were implanted bilaterally or unilaterally using quadripolar cylindrical leads with 1.5 mm contact height and 0.5 mm inter-contact spacing (Medtronic Model 3389-40). Techniques for subthalamic lead implantation have been described previously³⁴. Proper localization within the STN was verified by eliciting movement-related single cell discharge patterns and by test stimulation of the STN lead using an external pulse generator³⁴. This portion of the surgery was identical to standard clinical protocols.

On one side of the brain only, the primary motor cortex was implanted with a quadripolar paddle-type lead with 12 mm² exposed surface area and 1 cm inter-contact distance

(Medtronic Resume II, model 3587A25), except for the first patient whose cortical lead was a cylindrical lead with 3 mm contact height and 4 mm inter-contact spacing (Medtronic Model 3391-40). The cylindrical cortical lead was utilized only until regulatory approval for investigational use of the Resume II paddle lead in the subdural space was granted. The cortical lead was passed through the same 15 mm frontal burr hole used for the STN lead, but was directed posteriorly in the subdural space under fluoroscopic guidance such that at least one contact covered the arm area of primary motor cortex, on the medial aspect of the hand knob⁴⁰, approximately 3 cm from midline. Adequate anatomical localization of the cortical electrode array was confirmed using intraoperative CT computationally merged to the preoperative MRI in Framelink 5.0 (Stealthstation, Medtronic)³¹.

Functional localization of the cortical lead was verified by reversal of the N20 waveform of the somatosensory-evoked potential (SSEP, frequency 2 Hz, pulse width = 200 μ s, pulse train length = 160 s, amplitude = 25–40 mAmp), as has been previously reported⁶. If time permitted, a movement task described previously^{8,29} was also performed to ensure that canonical movement-related beta (13–30 Hz) power decreases and gamma (70–200 Hz) power increases were produced^{4,5,18}.

Subthalamic leads were secured to the skull using a standard lead anchoring device (Medtronic Stim-loc). On the brain side implanted with a cortical lead, the lead exited the burr hole in a bone trough underneath the Stim-loc base ring, and was secured to the skull with a titanium “dogbone” miniplate (Figure 1). After removal of the head-frame and induction of general anesthesia, a 3 cm parietal incision was made through which the free ends of the STN and cortical leads were accessed. These were attached to 40 cm lead extenders specifically designed to be used with the PC+S generator (Medtronic model 3708740). The extenders were tunneled to an infraclavicular incision and attached to the PC+S pulse generator/recording unit, which was placed in a pocket over the pectoralis muscle. If bilateral therapy was clinically indicated, a second STN electrode was implanted and attached to an Activa SC unit, placed in an infraclavicular pocket contralateral to Activa PC+S. The Activa SC only delivered therapeutic stimulation only, without a sensing capability.

Patient Visits

For most patients, study visits with brain recordings were performed 1 day, 10 days, 3 weeks, 1 month, 2 months, 3 months, 6 months and 1 year after surgery. (For patient 1, the recordings at 1 day, 2 months, and 3 months were not obtained; subsequent modification of our protocol allowed the additional recordings in patients 2–5). During research visits brain recordings were performed on and off medications and/or on and off DBS. Most visits were paired with a clinical appointment with a movement disorders neurologist. Programming for chronic therapeutic DBS was initiated during the one-month visit. For research-only visits (no clinical appointment), patients had the option of requesting that the research team come to their home for the recordings.

Initiating Recordings in Clinic

Recordings were triggered by placing the Sensing Programmer Telemetry Module (SPTM) over the patient’s chest at the site of the Activa PC+S implantation. The Sensing

Programmer (model 8181) was then used to initiate recordings. Recordings were either set to last for a specified duration or were manually terminated.

Home recordings

In addition to recordings during formal study visits, patients could also trigger brief recordings at home at any time, using the Medtronic Intercept patient programmer (model 37441). Patients were instructed how to initiate and verify recordings via a series of button presses prompted by the programmer screen. After the recording was initiated, the patient could remove the programmer from the chest. In our protocol, recording duration was pre-programmed by study personnel to be 1 minute.

Home recordings allowed patients to capture symptoms not easily recreated in the clinic and to acquire data in a more naturalistic setting. Patients were instructed to trigger recordings when they were experiencing any symptoms they thought were particularly severe, side effects from therapy, or during periods when they felt especially good. They were also asked to take notes about their experiences during each recording, as well as time since last the medication dose.

Recording Parameters

We utilized the highest sampling rate available (800 Hz) since we were particularly interested in examining activity in the higher frequency range. We performed short duration recordings (less than 9 minutes, repeated 1–3 times) at each research visit. Two channels of time series recordings were obtained simultaneously. For the majority of our recordings, we sampled 1 bipolar contact pair over primary motor cortex and 1 bipolar contact pair in STN, both in the time domain.

The selection of active cortical recording contacts was based on the pair showing the clearest somatosensory evoked potential N20 reversal, the strongest movement-related high gamma response, and/or strongest beta peak in the power spectrum, at the time of initial surgical insertion. We then verified that contacts with the strongest beta peak remained stable shortly after surgery using recordings with the Activa PC+S. Typically there was agreement between these criteria. When ambiguity remained, the preoperative MRI merged to the postoperative CT was used to help select an optimal contact pair for most recordings, based on closest proximity to the posterior precentral gyrus. Additional recordings with other contacts were sometimes performed, particularly if more than one contact pair had shown strong movement-related signals as described above. The selection criteria for the STN recording configuration differed before and after therapeutic DBS was activated. Prior to stimulation, we selected the bipolar pair whose LFP power spectrum showed the largest beta peak the day of or day after surgery, off of anti-parkinsonian medications. If selection was ambiguous, the center contacts (1–2) were used. After initiation of chronic therapeutic stimulation at one month, the contacts on either side of the stimulation contacts, when available, were used to minimize artifact. Note that our protocol stipulated that recordings on DBS would utilize each patient's clinical settings, and that therapeutic settings would be determined based on clinical criteria without consideration for optimal research recording settings. Thus, in many cases, our DBS settings were not optimal for recordings during

stimulation, particularly in STN where stimulation has a bigger impact on the occurrence of stimulation artifact²⁷.

Initially we recorded data without the use of optional additional digital filters. However, because we observed that saturation of STN sometimes occurred during DBS at therapeutic voltages, we later utilized a 100 Hz low pass filter (1 pole, RC). This filter was used for all recordings (both on and off DBS) for consistency.

Behavioral states

At each research visit and in each medication or stimulation state, brain recordings were performed in several different behavioral states including at rest, during walking, and during an iPad reaching task, which has been previously described^{8,29} and summarized below. Recording duration was 1–2 minutes for rest and walking files, and up to 6 minutes for the iPad task.

Assessing Signal Stability

To assess longitudinal signal stability, for each study visit we calculated root mean squared (RMS) voltage for both the STN LFP and motor cortex ECoG potentials. For this assessment, we used only resting recordings collected in clinic, when patients were off both DBS and medications (except for patient 1 who had great difficulty tolerating the off medication state, and so maintained her regular medication regimen at her 10 day, 6 month, and 1 year visits). If more than one file met these specifications for each visit, RMS was calculated for each recording separately and then averaged across recordings to obtain 1 value per brain region at each time point. For STN recordings we also omitted files contaminated by electrocardiogram (EKG) artifact (see *Results*, missing STN data in Figure 3B and 4, and Quinn et al 2015.) This artifact was avoidable by excluding contact zero from the recording configuration²⁷.

We also assessed signal stability by calculating both beta and gamma power for motor cortex ECoG and STN LFP over time. We calculated power spectral density (PSD) using the Welch method in Matlab (pwelch, 512 ms window, 1024 FFT length, and no overlap). For beta we averaged the log PSD between 13–30. For gamma we averaged log PSD in the broadband gamma range (70–100 Hz), avoiding potential line noise at 60 Hz and its first harmonic at 120 Hz.

We also calculated the height of the beta peak normalized to baseline power using a previously described method³⁷. In brief, the log of the PSD was taken and fit to a 5th order polynomial to approximately remove the 1/f component of the PSD²⁵. The largest local peak in the beta range (13–30 Hz) was then found, and the height was calculated. Sometimes this local maximum was small and not readily distinguishable from neighboring spectra. Therefore, data were also visually inspected to determine a threshold for reliable detection.

For these longitudinal analyses of spectral power, the recordings included were the same as those included in the RMS analysis described above. Again in recording sessions where multiple resting state data recordings were available, the PSD (for beta and gamma individually) or beta peak height was calculated for each recording, and averaged.

Reaching Task

Recording Paradigm—The reaching paradigm consisted of a “hold” period with the patient’s hand resting in their lap, then a cue indicating movement would soon begin, followed by a “go” cue and several seconds of continuous movement⁸. The exact timing of the stimulus delivery differed depending on patient reaction time and available time for data collection, but always contained a minimum of 5 seconds prior to movement and 2 seconds of continuous movement for each trial. Twenty trials were performed for each session.

During the reaching task, electromyography and accelerometry were recorded with an external recording system to determine movement onsets (Biosemi Active 2). In order to synchronize these data with the iPad task, an audio cable was connected between the two, and a brief auditory beep was played at the start of each trial. (Since the audio signal was fed directly from the iPad to the Biosemi external recording unit, the beep was not audible to the patient.) This synchronized the task to the external recording system as described previously^{8,29}. To synchronize the external recording system to Activa PC+S, surface electrical stimulation was used to deliver 0.2 ms periodic pulses. Conductive pads were placed on the patient’s head (near the forehead, but taking care to avoid large muscle groups to prevent uncomfortable muscle contractions during stimulation), and on the chest, near the implanted pulse generator (IPG). A train of pulses was then delivered at both the beginning and end of the task. During the train of pulses the frequency of the pulse train was changed (from 1 Hz to 2 Hz and then back to 1 Hz or vice versa). This improved the ability to synchronize the pulse artifacts from both recording systems, since occasional pulses were missed due to short pulse width. The goal was to produce a stimulation artifact that could be seen from both recording systems, so we delivered the stimulation at relatively high current (~10 mA), provided that it did not produce discomfort.

Analysis—We analyzed all recordings during the iPad reaching task to determine the presence of canonical movement-related activity: beta amplitude decreases and gamma amplitude increases^{2,4,5,18}. Raw signals were visually inspected and trials contaminated by artifact were excluded. Raw data were then filtered between 13–30 Hz for beta and 70–100 Hz for gamma, using a 2 way FIR 1 filter (‘eegfilt’ from the eeglab⁹ toolbox, with ‘fir1’ parameters). The Hilbert transform of the filtered signal was then calculated and the absolute value of this transform was obtained to derive the analytic amplitude over time in each frequency range. Spectrograms were also generated for visualization using the same approach but filtering all frequencies from 5 to 250 with a 2 Hz bandwidth.

Changes during movement were determined by aligning data from all trials relative to the time of the movement onset (time zero) and averaging across trials. The averaged amplitude was then normalized by a 500 ms baseline prior to movement onset (–2500 to –2000 ms relative to movement). Data were normalized by subtracting the average baseline amplitude and dividing by the baseline standard deviation. This ‘z-score’ procedure was performed separately for each frequency.

Recordings were categorized as having a detectable beta change if the z-scored values in the beta range (13 to 30 Hz) were at or below –1.96 (corresponding to a p-value of $p < 0.05$, uncorrected) for more than 150 ms during the time period from 500 ms before to 1 second

after movement initiation. This is a relatively liberal threshold (with no correction for multiple comparisons), since we were not trying to determine the effect of movement on electrophysiology (which is already well established^{4,5,18}), but instead to investigate the fidelity of the detection of this activity with the Activa PC+S.

An analogous procedure was performed for broadband gamma (70 to 100 Hz), except the threshold was set to a z-score value of 1.96 or above (since gamma increases are expected during movement). Since gamma detection can be difficult in STN (even in intraoperative recordings), an additional constraint was placed on the detection of gamma to avoid spurious detection associated with power increase across all frequencies. To avoid incorrectly categorizing these cases as true movement-related broadband gamma increases, a recording was only considered to have a reliable high gamma increase if there was also a beta power decrease. Visual inspection confirmed that this constraint avoided detection of these spurious gamma events. Thus this additional constraint was applied for all recordings (both STN and motor cortex).

Results

Subjects

Five patients (2 female/3 male) were enrolled and implanted. Patients were 47–62 years old at the time of surgery and had PD between 4–15 years (see Table 1 for details). Four of the five patients received bilateral DBS therapy, with the “non-research” side implanted with a quadripolar STN lead attached to an ipsilateral Activa SC single channel generator. Overall, patients were relatively heterogenous in terms of PD symptoms and severity.

Clinical Outcomes and adverse events

Four of five patients had improved motor function, indicated by reduced Unified Parkinson’s Disease Rating Scale (UPDRS) scores in the off medication state, as a result of DBS one year post-operatively (Table 2). One patient with minimal UPDRS improvement experienced rapid progression of symptoms post-implantation, and subsequently developed features consistent with multi-system atrophy, parkinsonian subtype (MSA-P). Another patient who was implanted with unilateral DBS experienced disease progression on the non-implanted side during study duration. However he did have a clinical benefit from DBS on the treated side. No patients reported any suicidal ideation or attempts during the study.

There were no serious adverse events related to the study protocol. Minor complications included development of a painless, nonerythematous postoperative subgaleal fluid collection near the burr hole on the side implanted with the cortical lead, presumed to be CSF, which was self limited; thinning of the skin over the Activa PC+S battery implantation which remained stable without need for surgical revision, and an episode of lightheadedness during programming which resolved with rest. Each of these occurred only once. Two protocol violations occurred: inadvertent performance of a postoperative MRI in one patient, without clinical sequelae, and an episode of inadvertent activation of cortical stimulation for 30–45 minutes, without clinical sequelae, in another patient.

Contact Localization

Cortical electrode arrays were successfully placed over left (3 subjects) and right (2 subjects) motor cortex and in ipsilateral STN in all subjects. See Figure 1 for example lead locations and Table 3 for AC-PC coordinates for cortical contacts and the STN lead tip, measured from intraoperative CT fused to the preoperative MRI. Comparison of intraoperative to postoperative CT (acquired between 3 weeks to 3 months after surgery) revealed that movement of the cortical electrode array was minimal, with less than 3.5 mm of movement in each case (mean 1.7 mm, range 0–3.5 mm).

Signal quality and stability over one year

The quality of recordings with Activa PC+S, off stimulation a few hours post implantation, was similar to those recorded intraoperatively with an FDA-approved external recording system designed for human electrophysiology (Microguide, Alpha Omega) (Figure 2), with the exception of some artifacts discussed further below. This comparison has also been made in nonhuman primates². As expected based on intraoperative recordings, signal amplitude of the STN LFP recorded with Activa PC+S was lower than the simultaneously recorded motor ECoG potentials⁷ (see examples in Figure 3A). The average RMS voltage at rest, off DBS was 5.1 (SD = 0.38) microvolts for STN and 20.4 (SD = 2.79) microvolts for motor cortex. These RMS values remained relatively stable over time (Figure 3B), although some patients did have an initial decrease in RMS shortly after surgery.

Despite this RMS signal stability, electrode impedances for both cortical and STN leads did increase over time (Figure 4E). However, this increase did not have a strong effect on the power of key frequency bands over time (see below).

Detection of physiologically important frequency bands

The presence of prominent oscillatory activity in the beta band (13–30 Hz) is expected in field potential recordings from brain structures in the motor system. Gamma band activity in the cortex, over a broad frequency range (50–200 Hz) is a useful marker of local cortical activation¹⁷. Log beta power (Figure 4A) and log gamma power at rest, off DBS (Figure 4B) varied between patients, but were relatively stable over time within subjects, especially after the first month, similar to observations in non-human primates². The amplitude of the PSD beta peak with respect to baseline power (see *Methods*) was more variable, but still there was not a systematic change in beta peak height over time (see Figure 4C–D). While a beta peak was usually present, there were several instances wherein a beta peak was not clearly detected, especially in STN. STN LFP recordings that lacked the expected beta peak have also been observed by other groups²⁰. Using our criteria for quantifying a beta peak in the power spectrum, a local maxima was always found in the beta range, but sometimes the height of this maxima was close to zero, suggesting that the peak was difficult to distinguish from the rest of the spectra. Visual inspection suggested that any beta peak values with a height of less than $0.25 \log_{10} (\mu V^2/Hz)$ (see Figure 4C–D) were difficult to distinguish from the rest of the spectrum, and likely unreliable (Figure 4F). Thirteen of 42 recordings (31%) in STN and 5 of 62 recordings (8%) in motor cortex met this criterion. Failure to detect a beta peak was more common in STN and was more common in a subset of patients (Table 4); one patient had unreliable beta peak detection in 71% of recordings, another in 60% of

recordings, while the other three had reliable beta peaks in most recordings. Only 2 of the 5 patients had any instances of unreliable beta peak detection in motor cortex.

Variable beta peak detection may be unrelated to Active PC+S recording capabilities. Beta oscillatory activity is known to dynamically change with behavior including movement and cognition^{5,24}, and in PD it is also affected by medication state¹³. Of note, our patient with the lowest rate of beta peak detection (Patient 3) was eventually diagnosed with multi-systems atrophy. Finally, differences in recording location in the STN region may also relate to differences in the strength of the beta peak³⁸.

Movement Related Changes

Examples of time-frequency plots showing movement related changes in motor cortex ECoG potentials, during the iPad-based arm movement task, are provided in Figure 5. For all such recordings, we classified beta power decreases and gamma power increases as present or absent (see *Methods*). Almost all motor cortex recordings (54/55, or 98%) had a beta power decrease at movement initiation, and most exhibited a gamma power increase (37/55, or 67%). Conversely, beta power changes in STN were more difficult to detect (34/49, or 69%) and gamma power changes were even more difficult (13/49, or 27%).

Proportions of recordings with detectable movement related changes in beta and gamma in individual subjects are provided in Table 5. For motor cortex, gamma power changes with movement are typically detected when recording ECoG potentials through externalized leads. Notably, a subset of patients (2, 4, and 5) also performed the same task intraoperatively with externalized motor cortex recordings. There were detectable movement related beta and gamma changes in these recordings for all three subjects, while 26% of their subsequent PC+S recordings did not have a movement related gamma increase. Thus we suspect reduced signal to noise in the high frequency relative to the Activa PC+S noise floor may explain the lack of detection (Figure 5C). Note that gamma power in STN is difficult to detect due to a smaller signal strength, and is often not detected even in intraoperative recordings. Thus, failure to detect it here is likely not specific to Activa PC+S recording characteristics.

The ability to detect beta and gamma band changes during therapeutic neurostimulation will be important for the eventual use of neural interfaces for feedback-controlled stimulation. During DBS, movement-related signals in motor cortex were still detectable at a similar level with 34/36 or 94% of recordings having detectable beta and 25/36 or 69% having detectable gamma. In STN, however, signal detection was much reduced with only 4/26 or 15% of recordings having detectable beta and 0/26 or 0% with detectable gamma (Table 5).

Accurate signal averaging of event-related neural activity over multiple repetitions of a task depends on correct event alignment. This depends on the consistency of data sampling rate over successive trials. We examined the consistency of the Activa PC+S sampling rate for all files with event-related activity (i.e. during iPad reaching task), using the synchronization procedure described in the *Methods* section, and found that it varied between 788 Hz to 794 Hz in extreme cases, and was typically between 792 and 794Hz, when the nominal sampling

rate was programmed at 800 Hz. Our synchronization procedure allowed us to calculate the sampling rate for each recording and improve time-locking precision.

Artifacts

Brain sensing during stimulation is one of the most technically challenging aspects of totally implantable brain recording systems, compared to intraoperative recording from externalized leads. During therapeutic stimulation, artifacts occurred at the stimulation frequency and also at its folded sub-harmonics (Figure 6A). Stimulation artifacts were more prominent for the STN LFP than ECoG potentials, given the smaller signal amplitude as well as the proximity of the stimulation source to the recording array. For cortical recording, detection of canonical movement related changes in beta and gamma bands during DBS was similar to when DBS was off, whereas for STN recordings, DBS reduced the fidelity of detection of event related changes (Table 5). In general, stimulation artifacts arise from two main sources: volume conduction through the brain, and coupling between the stimulation and recording circuits with stimulation/sensing device. While the former can be greatly reduced by signal detection at a distance from the stimulating electrode, the latter (Figure 6) is more prominent than is the case for similar recordings from externalized leads connected to large external amplifiers⁸, for which isolation of stimulation and recording circuits is technically simpler.

Several narrowband artifacts were also present in Activa PC+S recordings even when stimulation was off. The frequency of these artifacts depended on the sampling rate utilized. At 800 Hz the most obvious of these artifacts occurred at 200 Hz and 32 Hz (see Figure 6B). The origin of the 200 Hz artifact (based on communication from Medtronic engineers) is an internal firmware processing step performed on every 4th data sample, creating an artifact at the sampling rate divided by 4. The 32 Hz artifact is due to an internal Activa PC+S clock which is present to allow for configuration of each channel as a power channel (in addition to a time domain channel). This clock artifact interacts with the sampling rate to create an artifact at 32 Hz (when sampling at 800 Hz). Avoiding analysis of these frequencies can prevent misinterpretation of the data. This is typically straightforward for 200 Hz, but is more difficult for 32 Hz, since it is close to beta, an important frequency band in the motor system and in movement disorders^{5,10}. When signal amplitude is low, this artifact could mimic or obscure physiological beta (Figures 3, 4, and 6). High amplitude signals, like those recorded from motor cortex or STN recordings with a robust LFP (Figure 4F), are not strongly influenced.

STN recordings from contact 0 (the most ventral contact) usually had electrocardiogram (EKG) contamination (Figure 6C). This is believed to originate from current leakage into the IPG at the insertion site of the device lead extenders over the pectoralis muscle. Medtronic engineers have proposed a solution involving sealant at the lead extender-pulse generator interface²⁷. We also observed baseline deflections in the signal at the initiation of recordings. This sensing channel start-up transient, decayed back to zero volts over 3–10 seconds (Figure 6D). Another type of transient baseline deflection observed was sudden “jumps” in voltage, followed by decay back to zero (Figure 6E). These occurred infrequently, mainly in home recordings, and may be due to head movements. Both these

artifacts are brief, so excluding portions of the signal with baseline shifts is sufficient to avoid an impact on data analysis. Of note, 60 Hz line noise and its harmonics were not prominent, as is expected based on the isolation of a totally implantable device from external sources of noise.

Data Downloads

Data downloads were performed 1–3 times during research visits, and required a minimum of 17–18 minutes (when memory was full). However, downloading time was extended during episodes of telemetry loss between the sensing programmer and PC+S, usually associated with voluntary or involuntary movements. Disconnections required readjustment of the sensing programmer antenna. Cancelling a download already in progress was not useful, as it often resulted in freezing of the sensing tablet, requiring a hard restart.

Discussion

We utilized a novel, investigational, totally implantable, bidirectional neural interface to record motor cortex ECoG potentials and STN LFPs in 5 PD patients over 1 year. There were no serious surgical complications, no unintended interruptions in DBS therapy, and no major malfunction of the recording features of the device. Signal amplitudes in both cortex and STN (measured as both RMS voltage and detection of beta and gamma power) remained relatively stable over time, in spite of an increase in average monopolar contact impedances over time in both regions. In motor cortex, the canonical movement-related beta frequency decrease⁵ was reliably detected, the movement related high gamma increase⁴ was seen in 2/3 of recordings, and therapeutic stimulation did not preclude detection. STN detection of movement related gamma changes was less reliable, and more strongly influenced by stimulation artifact. The STN LFP signal can, however, be improved by utilizing specific stimulation and recording configurations. These findings should be of use to investigators planning research protocols using PC+S, as well as to device companies designing the next generation of bidirectional neural interfaces.

Neural Interfaces for Invasive Recording in Humans

Activa PC+S is one of few chronic invasive recording devices available for human use. Others are the Responsive Neurostimulation (RNS) device (*Neuropace, Inc.*)^{21,35}, designed for epilepsy treatment, and the BrainGate device (*Braingate Co.*), a brain machine interface designed for patients with paralysis^{12,36}. While all three of these devices allow invasive electrophysiologic recording, there are important differences, advantages, and limitations to each. Both RNS and Activa PC+S are fully internalized devices while BrainGate has an externalized component. The internalized devices have the significant advantage of reduced risk of infection and capability for ambulatory recording outside of a specialized laboratory, at the expense of limited bandwidth. The BrainGate system, in contrast, allows recording from far more electrodes as well as high sampling rates that allow for detection of single unit activity in addition to field potentials.

Both BrainGate and Activa PC+S allow rapid, immediate, streaming of data to external computers, facilitating brain-machine interface applications such as real time control of a

motor prosthesis^{12,36}. Activa PC+S can also be used to prototype feedback-controlled DBS algorithms, guided either by brain recording, or external sensors¹⁵. Feedback control may improve DBS therapy by real time-adjustment of stimulation parameters in response to fluctuating signs and symptoms^{14,28}. The possible reduction in stimulation current, and associated improved battery life, must be balanced against the potential for increased energy use associated with continuous data sensing³⁰.

Of the available implantable devices with a sensing capability, Activa PC+S is the only one designed for continuous stimulation, and thus is suitable to deliver therapy for any disorder treatable with open-loop DBS¹⁹. The use of Activa PC+S in humans with PD for *single site*, subcortical recording, with continuous stimulation was recently reported^{20,27}. Here we present the first use of PC+S in humans that utilizes a multi-site recording configuration (cortex and basal ganglia).

Device limitations and mitigation strategies

Many of the technical limitations of Activa PC+S are due to the constraints associated with integrating the sensing function into an implantable device with high current drain from therapeutic stimulation, in comparison with research grade systems for human recording through externalized electrodes. Thus, high frequency activity such as the canonical movement related high gamma changes in motor cortex, reliably detected using externalized ECoG arrays^{4,5,18,29}, were not always detectable using PC+S. The optimal frequencies for gamma power detection are above 70 Hz, for which signal amplitudes are near or below the device noise floor of PC+S in some patients (see Figure 5C). High gamma (also called broadband gamma) activity tracks local cortical function and is thought to be a surrogate for local neural activity¹⁷. Further, cross frequency interactions between the amplitude of high gamma and the phase of lower frequency rhythms may provide important control signals for adaptive (closed loop) stimulation^{7,8}, underscoring the importance of high gamma sensing. For some subjects in this study, cortical gamma detection was reliable over the one year study duration, but further improvement in noise performance in future generation devices will be important for high gamma sensing in subjects who may have lower signal amplitude.

Stimulation artifact is more pronounced with Activa PC+S than when stimulating and recording from externalized leads⁸. This is probably due to coupling of the stimulation and recording circuits within the pulse generator. The stimulation artifact is particularly challenging in STN, where it can make detection of beta power less reliable, create artifacts in frequency ranges that are potentially important, and in some cases totally saturate the signal (Figure 6A). This may limit the feasibility of close-loop DBS approaches using STN LFP beta power as a control signal¹⁴. Stimulation artifacts may be reduced by use of the 100 Hz low pass filter. Use of constant voltage rather than constant current stimulation aides in common mode rejection of stimulation artifacts. Stimulation frequency may be selected judiciously so as to align stimulation artifacts away from the frequency bands of interest (For example, 140 Hz stimulation results in artifacts above 130 Hz or below 10 Hz, away from the frequency bands of greatest interest for many applications). Recording from a bipolar configuration that brackets a monopolar stimulating contact is ideal for artifact reduction, but this may not be possible if the clinically optimal stimulation contact is on one

end of the contact array. Finally, a calibration procedure can be performed prior to each recording to determine optimal STN gain²⁷.

Fully implantable devices pose a trade-off between device recording capability and the longevity of the power supply. Our protocol used the highest sampling rate, recording of 2 time domain signals, and no data compression. These settings are among the most demanding with respect to memory capacity, permitting approximately 9 minutes of data storage prior to download. Because of this, we performed multiple data recording and download sessions within most study visits. Memory capacity in Activa PC+S can be improved by using data compression (although this is not recommended during DBS), lowering the sampling rate, recording in the power domain at a specified frequency instead of time domain, and by sampling fewer channels.

Characterizing the variability in sampling rate was critical for analysis of task-related activity, since this variability affects precise event alignment when signal averaging over multiple trials. Without changing the nominal programmed sampling rate, actual sampling rate can vary between patients and between recording sessions within a patient. To address this, we delivered synchronization pulses at the beginning and end of each task recording, and calculated sampling rate from the number of samples collected and the length of the interval between pulses. For longer recordings, additional synchronization pulses may be necessary.

Conclusions

We report our initial experience with subcortical neurostimulation combined with chronic cortical and subcortical recording for 1 year in five PD patients using a bidirectional neural interface. The acquisition of high quality long-term ECoG and LFP data is achievable. For most disorders, brain network abnormalities underlying disease expression are yet to be discovered. Totally implantable sensing devices hold promise both for signal discovery and for feedback-controlled stimulation. These developments will be facilitated by improvements in signal-to-noise ratio, increased bandwidth and memory, reduced time for data downloading, and better methods of synchronizing internal data sampling with external monitors and computers.

Acknowledgments

We would like to thank Andrew Miller for his help with the cortical reconstruction shown in Figure 1C. This study was supported by the UC President's Postdoctoral fellowship (NCS), the NIH Neurological Disorders and Stroke (NINDS R01 NS090913-01, to PAS), and the Michael J Fox Foundation (CDH).

References

1. Afshar P, Khambhati A, Stanslaski S, Carlson D, Jensen R, Linde D, et al. A translational platform for prototyping closed-loop neuromodulation systems. *Front Neural Circuits*. 2012; 6:117. [PubMed: 23346048]
2. Connolly AT, Muralidharan A, Hendrix C, Johnson L, Gupta R, Stanslaski S, et al. Local field potential recordings in a non-human primate model of Parkinsons disease using the Activa PC + S neurostimulator. *J Neural Eng*. 2015; 12:066012. [PubMed: 26469737]

3. Constantoyannis C, Berk C, Honey CR, Mendez I, Brownstone RM. Reducing hardware-related complications of deep brain stimulation. *Can J Neurol Sci.* 2005; 32:194–200. [PubMed: 16018154]
4. Crone NE, Miglioretti DL, Gordon B, Lesser RP. Functional mapping of human sensorimotor cortex with electrocorticographic spectral analysis. II. Event-related synchronization in the gamma band. *Brain.* 1998; 121(Pt 12):2301–2315. [PubMed: 9874481]
5. Crone NE, Miglioretti DL, Gordon B, Sieracki JM, Wilson MT, Uematsu S, et al. Functional mapping of human sensorimotor cortex with electrocorticographic spectral analysis. I. Alpha and beta event-related desynchronization. *Brain.* 1998; 121(Pt 12):2271–2299. [PubMed: 9874480]
6. Crowell AL, Ryapolova-Webb ES, Ostrem JL, Galifianakis NB, Shimamoto S, Lim DA, et al. Oscillations in sensorimotor cortex in movement disorders: an electrocorticography study. *Brain.* 2012
7. de Hemptinne C, Ryapolova-Webb ES, Air EL, Garcia PA, Miller KJ, Ojemann JG, et al. Exaggerated phase-amplitude coupling in the primary motor cortex in Parkinson disease. *Proc Natl Acad Sci U S A.* 2013; 110:4780–4785. [PubMed: 23471992]
8. de Hemptinne C, Swann NC, Ostrem JL, Ryapolova-Webb ES, San Luciano M, Galifianakis NB, et al. Therapeutic deep brain stimulation reduces cortical phase-amplitude coupling in Parkinson's disease. *Nat Neurosci.* 2015; 18:779–786. [PubMed: 25867121]
9. Delorme A, Makeig S. EEGLAB: an open source toolbox for analysis of single-trial EEG dynamics including independent component analysis. *J Neurosci Methods.* 2004; 134:9–21. [PubMed: 15102499]
10. Hammond C, Bergman H, Brown P. Pathological synchronization in Parkinson's disease: networks, models and treatments. *Trends Neurosci.* 2007; 30:357–364. [PubMed: 17532060]
11. Herrington TM, Cheng JJ, Eskandar EN. Mechanisms of deep brain stimulation. *J Neurophysiol.* 2016; 115:19–38. [PubMed: 26510756]
12. Hochberg LR, Serruya MD, Friehs GM, Mukand JA, Saleh M, Caplan AH, et al. Neuronal ensemble control of prosthetic devices by a human with tetraplegia. *Nature.* 2006; 442:164–171. [PubMed: 16838014]
13. Kühn AA, Kupsch A, Schneider G-H, Brown P. Reduction in subthalamic 8–35 Hz oscillatory activity correlates with clinical improvement in Parkinson's disease. *Eur J Neurosci.* 2006; 23:1956–1960. [PubMed: 16623853]
14. Little S, Pogosyan A, Neal S, Zavala B, Zrinzo L, Hariz M, et al. Adaptive deep brain stimulation in advanced Parkinson disease. *Ann Neurol.* 2013; 74:449–457. [PubMed: 23852650]
15. Malekmohammadi M, Herron J, Velisar A, Blumenfeld Z, Trager MH, Chizeck HJ, et al. Kinematic Adaptive Deep Brain Stimulation for Resting Tremor in Parkinson's Disease. *Mov Disord.* 2016; 31:426–428. [PubMed: 26813875]
16. Mann JM, Foote KD, Garvan CW, Fernandez HH, Jacobson CE, Rodriguez RL, et al. Brain penetration effects of microelectrodes and DBS leads in STN or GPi. *J Neurol Neurosurg Psychiatry.* 2009; 80:794–797. [PubMed: 19237386]
17. Manning JR, Jacobs J, Fried I, Kahana MJ. Broadband shifts in local field potential power spectra are correlated with single-neuron spiking in humans. *J Neurosci.* 2009; 29:13613–13620. [PubMed: 19864573]
18. Miller KJ, Leuthardt EC, Schalk G, Rao RPN, Anderson NR, Moran DW, et al. Spectral Changes in Cortical Surface Potentials during Motor Movement. *Journal of Neuroscience.* 2007; 27:2424–2432. [PubMed: 17329441]
19. Miocinovic S, Somayajula S, Chitnis S, Vitek JL. History, applications, and mechanisms of deep brain stimulation. *JAMA Neurol.* 2013; 70:163–171. [PubMed: 23407652]
20. Neumann WJ, Staub F, Horn A, Schanda J, Mueller J, Schneider GH, et al. Deep Brain Recordings Using an Implanted Pulse Generator in Parkinson's Disease. *Neuromodulation.* 2016; 19:20–24. [PubMed: 26387795]
21. Okun MS, Foote KD, Wu SS, Ward HE, Bowers D, Rodriguez RL, et al. A trial of scheduled deep brain stimulation for Tourette syndrome: moving away from continuous deep brain stimulation paradigms. *JAMA Neurol.* 2013; 70:85–94. [PubMed: 23044532]
22. Oswal A, Brown P, Litvak V. Synchronized neural oscillations and the pathophysiology of Parkinson's disease. *Curr Opin Neurol.* 2013; 26:662–670. [PubMed: 24150222]

23. Panov F, Levin E, de Hemptinne C, Swann N, Qasim S, Miocinovic S, et al. Intraoperative electrocorticography for physiological research in movement disorders: principals and experience in 200 cases. *Journal of Neurosurgery*. 2016 in press.
24. Pfurtscheller G. Central beta rhythm during sensorimotor activities in man. *Electroencephalogr Clin Neurophysiol*. 1981; 51:253–264. [PubMed: 6163614]
25. Pritchard WS. The brain in fractal time: 1/f-like power spectrum scaling of the human electroencephalogram. *Int J Neurosci*. 1992; 66:119–129. [PubMed: 1304564]
26. Qasim SE, de Hemptinne C, Swann NC, Miocinovic S, Ostrem JL, Starr PA. Electrocorticography reveals beta desynchronization in the basal ganglia-cortical loop during rest tremor in Parkinson's disease. *Neurobiol Dis*. 2015
27. Quinn EJ, Blumenfeld Z, Velisar A, Koop MM, Shreve LA, Trager MH, et al. Beta oscillations in freely moving Parkinson's subjects are attenuated during deep brain stimulation. *Mov Disord*. 2015; 30:1750–1758. [PubMed: 26360123]
28. Rosin B, Slovik M, Mitelman R, Rivlin-Etzion M, Haber Suzanne N, Israel Z, et al. Closed-Loop Deep Brain Stimulation Is Superior in Ameliorating Parkinsonism. *Neuron*. 2011; 72:370–384. [PubMed: 22017994]
29. Rowland NC, De Hemptinne C, Swann NC, Qasim S, Miocinovic S, Ostrem JL, et al. Task-related activity in sensorimotor cortex in Parkinson's disease and essential tremor: changes in beta and gamma bands. *Front Hum Neurosci*. 2015; 9:512. [PubMed: 26441609]
30. Ryapolova-Webb E, Afshar P, Stanslaski S, Denison T, de Hemptinne C, Bankiewicz K, et al. Chronic cortical and electromyographic recordings from a fully implantable device: preclinical experience in a nonhuman primate. *J Neural Eng*. 2014; 11:016009. [PubMed: 24445430]
31. Shahlaie K, Larson PS, Starr PA. Intraoperative computed tomography for deep brain stimulation surgery: technique and accuracy assessment. *Neurosurgery*. 2011; 68:114–124. discussion 124. [PubMed: 21206322]
32. Stanslaski S, Afshar P, Cong P, Giftakis J, Stypulkowski P, Carlson D, et al. Design and validation of a fully implantable, chronic, closed-loop neuromodulation device with concurrent sensing and stimulation. *IEEE Trans Neural Syst Rehabil Eng*. 2012; 20:410–421. [PubMed: 22275720]
33. Stanslaski S, Cong P, Carlson D, Santa W, Jensen R, Molnar G, et al. An implantable bidirectional brain-machine interface system for chronic neuroprosthesis research. *Conf Proc IEEE Eng Med Biol Soc*. 2009; 2009:5494–5497. [PubMed: 19965049]
34. Starr PA, Christine CW, Theodosopoulos PV, Lindsey N, Byrd D, Mosley A, et al. Implantation of deep brain stimulators into the subthalamic nucleus: technical approach and magnetic resonance imaging-verified lead locations. *J Neurosurg*. 2002; 97:370–387. [PubMed: 12186466]
35. Sun FT, Morrell MJ. The RNS System: responsive cortical stimulation for the treatment of refractory partial epilepsy. *Expert Rev Med Devices*. 2014; 11:563–572. [PubMed: 25141960]
36. Truccolo W, Friehs GM, Donoghue JP, Hochberg LR. Primary motor cortex tuning to intended movement kinematics in humans with tetraplegia. *J Neurosci*. 2008; 28:1163–1178. [PubMed: 18234894]
37. Wang DD, de Hemptinne C, Miocinovic S, Qasim SE, Miller AM, Ostrem JL, et al. Subthalamic local field potentials in Parkinson's disease and isolated dystonia: An evaluation of potential biomarkers. *Neurobiol Dis*. 2016
38. Weinberger M, Mahant N, Hutchison WD, Lozano AM, Moro E, Hodaie M, et al. Beta oscillatory activity in the subthalamic nucleus and its relation to dopaminergic response in Parkinson's disease. *J Neurophysiol*. 2006; 96:3248–3256. [PubMed: 17005611]
39. Wichmann T, DeLong MR. Basal ganglia discharge abnormalities in Parkinson's disease. *J Neural Transm Suppl*. 2006:21–25. [PubMed: 17017504]
40. Yousry TA, Schmid UD, Alkadhi H, Schmidt D, Peraud A, Buettner A, et al. Localization of the motor hand area to a knob on the precentral gyrus. A new landmark. *Brain*. 1997; 120(Pt 1):141–157. [PubMed: 9055804]

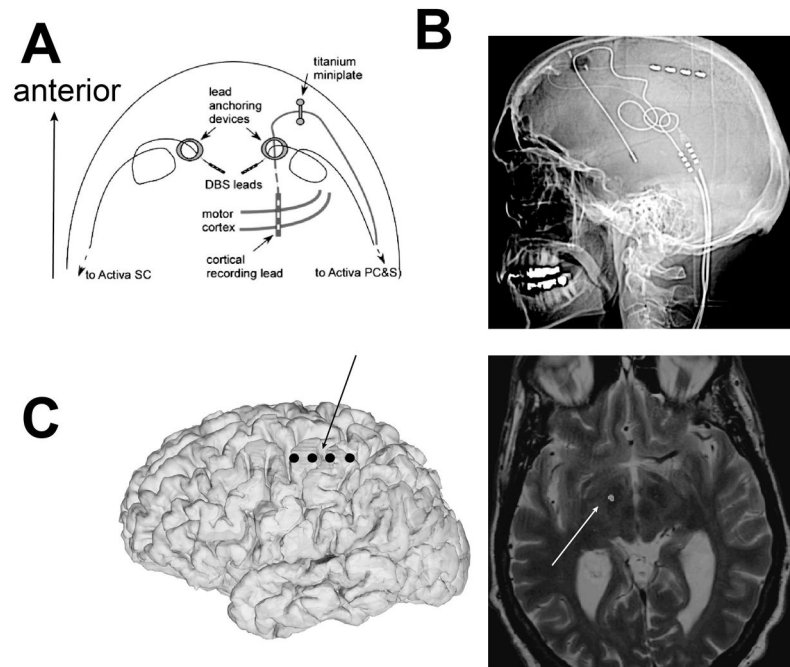


Figure 1.

A. Schematic of the cranial hardware implantation (bilateral brain leads) as viewed from the top of the head. B. Lateral skull film showing cranial hardware and proximal lead extenders. This subject has unilateral DBS. C. Example lead locations (patient 4). Central sulcus indicated with the black arrow and DBS electrode location in the subthalamic nucleus indicated with the white dot. Electrode locations determined by merging the pre-operative MRI to a postoperative CT.

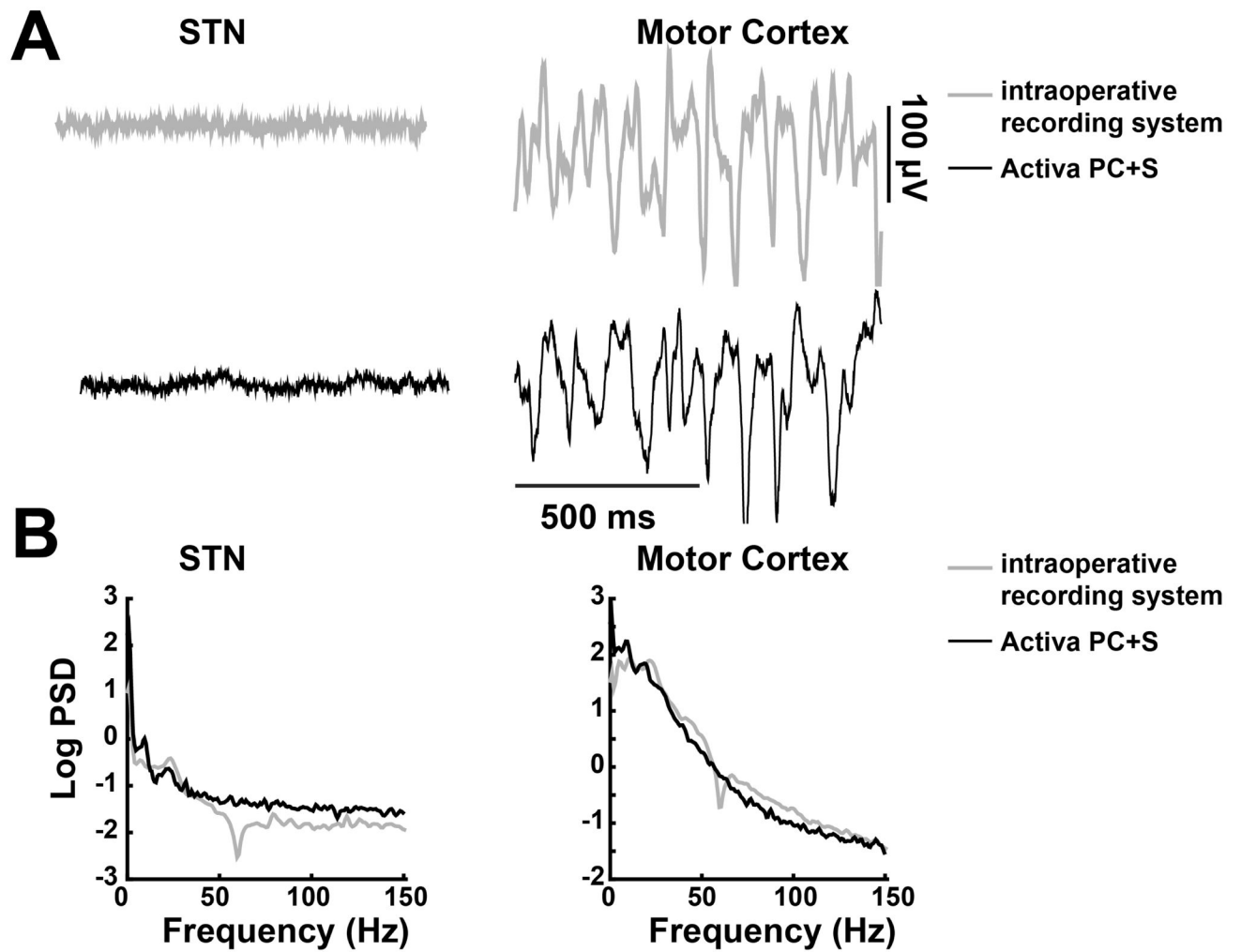


Figure 2. Example of motor cortex ECoG and STN LFP raw data (A) and their power spectra (B) from Activa PC+S versus an external recording system designed for intraoperative electrophysiology (*Microguide*, Alpha Omega). Both recordings were obtained on the same day, a few hours apart, from patient 5.

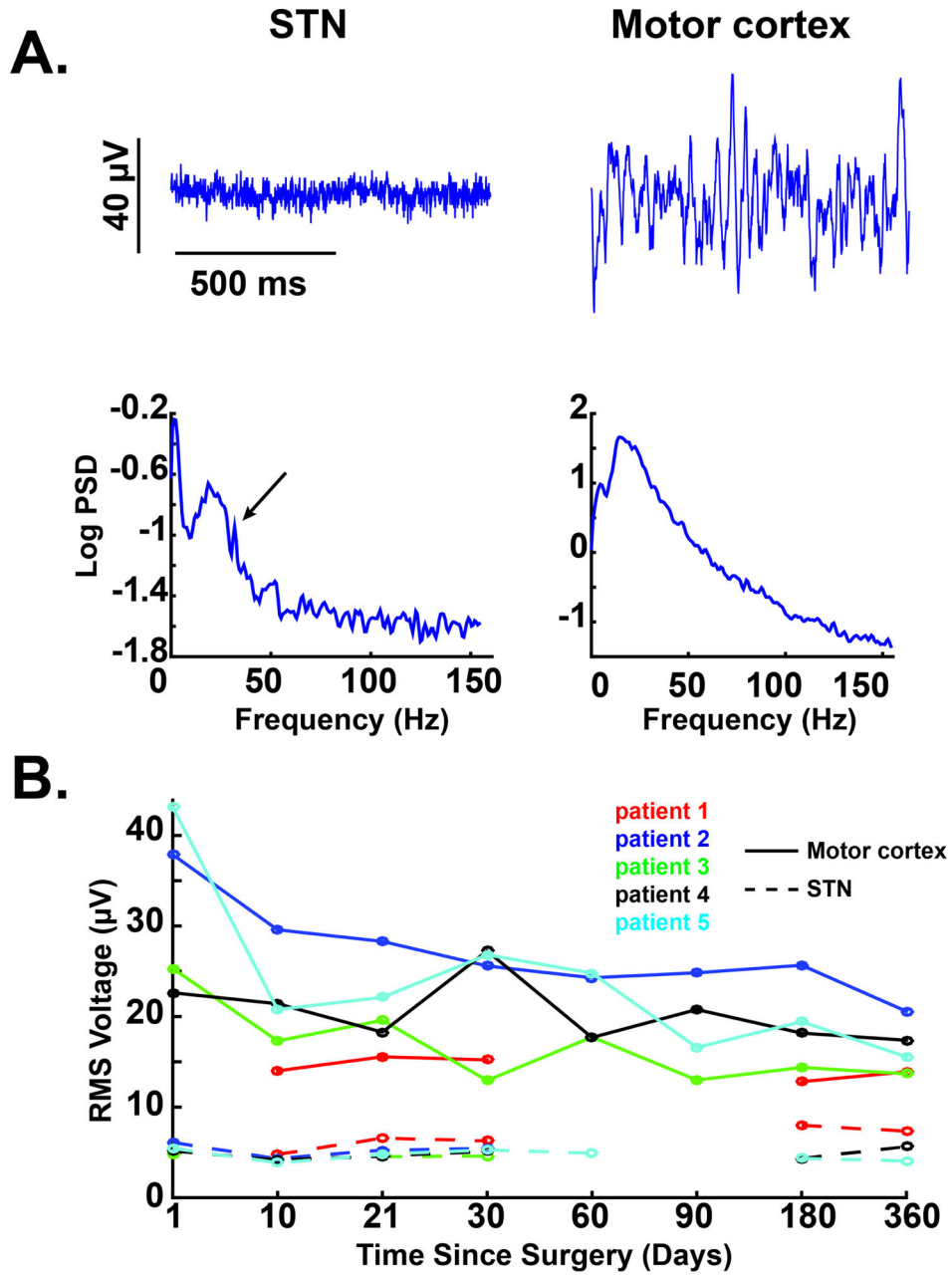


Figure 3. Signal quality and evolution over time. A. Example signals and their power spectra from patient 2, 10 day post-operative, for both STN (left panel) and motor cortex (right panel). On the STN PSD, the sharp peak at 32 Hz (arrow), on the right shoulder of the beta peak, is artifactual (further elaborated in Figure 6). B. Evolution of RMS voltage over time for all patients. Data for patient 1 at 1 day, 2 months, and 3 months is missing because the initial protocol did not include research visits at these time points. STN recordings which were contaminated by EKG artifact (see Figure 6) were also excluded.

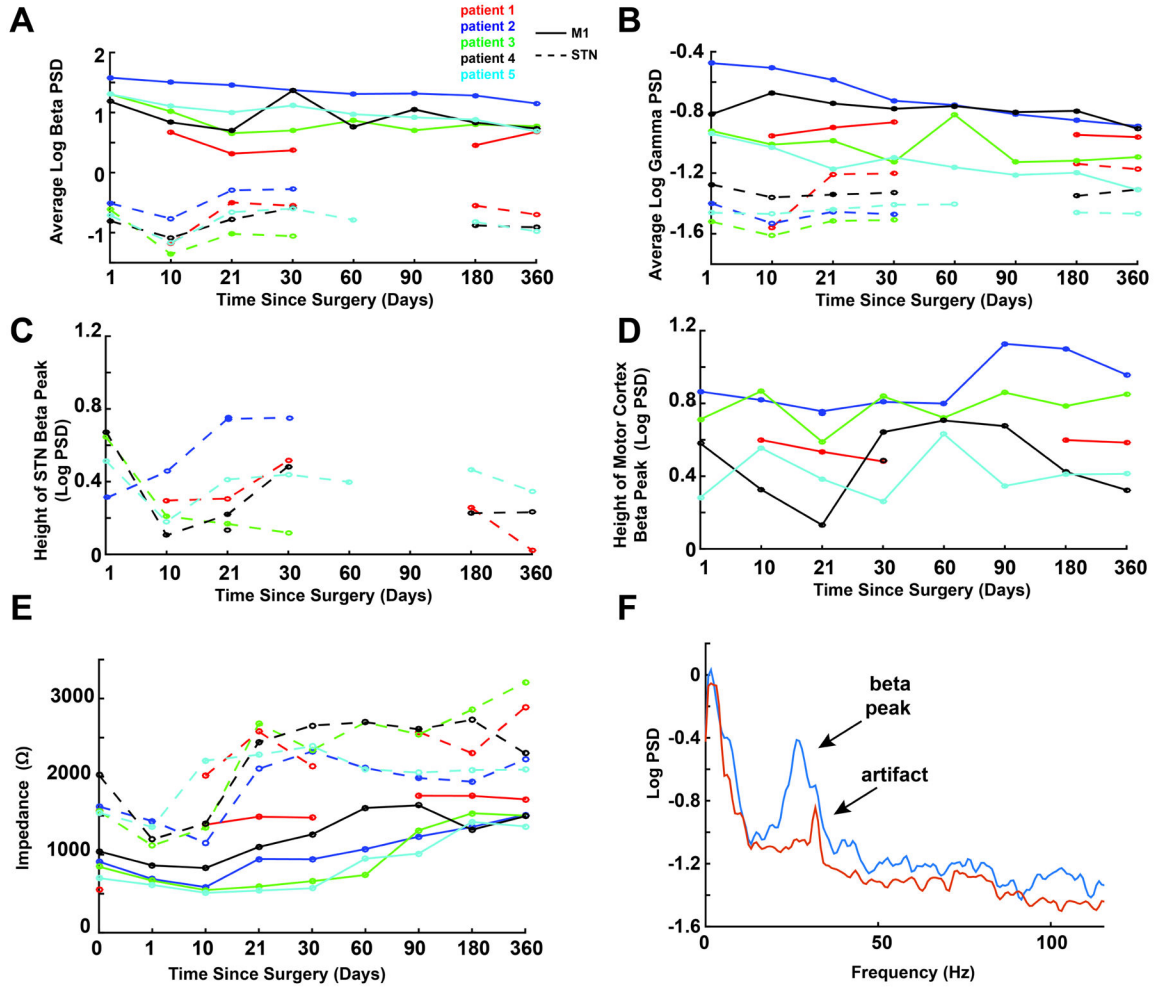


Figure 4. Power and impedance change over time. A. Average log beta PSD over time for all subjects. B. Average log broadband gamma over time for all subjects. C. Average log beta peak height in STN over time for all subjects. Data for patient 1 at 1 day, 2 months, and 3 months is missing because the initial protocol did not include research visits at these time points. Also STN recordings contaminated by EKG artifact (see Figure 6) were excluded. D. Same as C, but motor cortex beta peak height. E. Average monopolar impedances across all electrode contacts for each region (motor cortex and STN). Impedances gradually increase over time. F. Example of an STN LFP power spectrum with (patient 4, 1 day after surgery) and without (patient 4, 10 days after surgery) the expected broad peak in the alpha-beta range. Note that the sharp peak at 32 Hz from the 10 day post-surgery recording is an artifact (described further in *Results* and Figure 6).

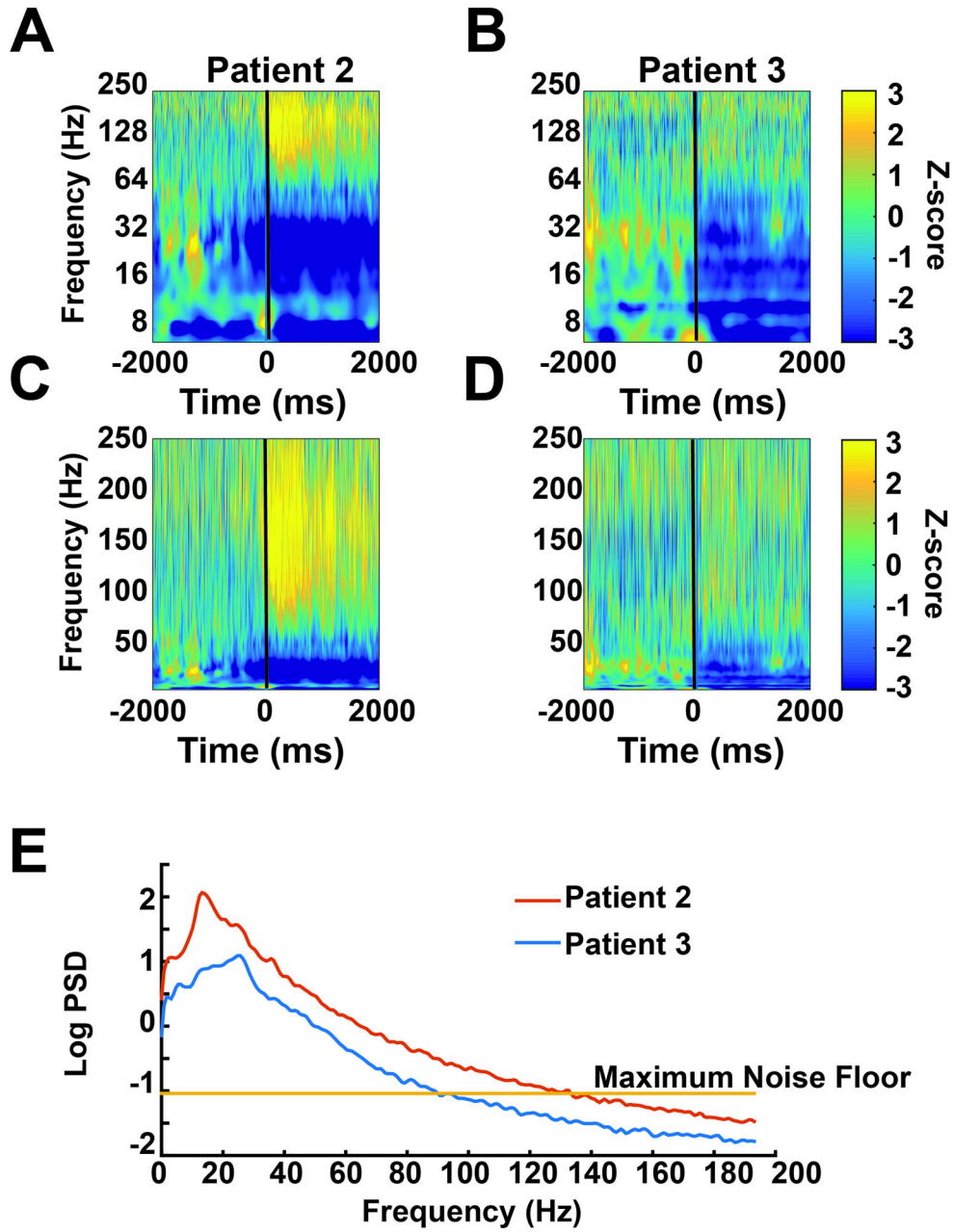
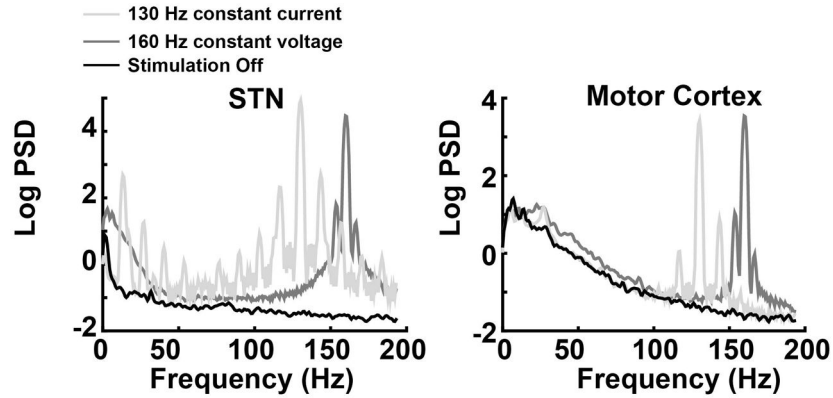
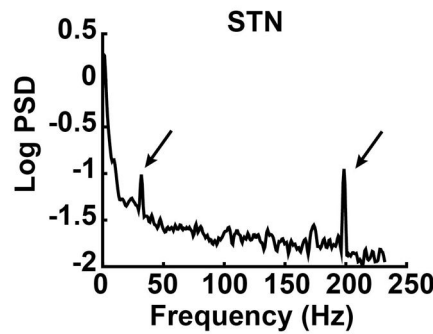


Figure 5. Detection of movement related changes in motor cortex ECoG potentials and their relationship to device noise floor. A, B: Movement related spectrograms (plotted on a log scale) aligned to movement onset (time 0) for a recording session that did (A, patient 2, 10 days postoperative) and did not (B, patient 3, 3 weeks postoperative) exhibit a movement-related gamma increase. Both examples have a beta decrease. D, C show the same plots on a non-log scale. E. PSD plots for recordings shown in A–D, as well as the maximum manufacturer-specified device noise floor. Note that gamma activity may be difficult to detect reliably in panels B and D because gamma activity in that recording is near the device noise floor.

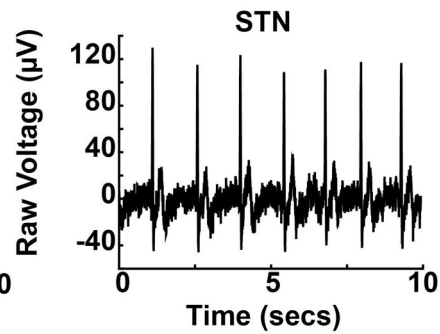
A. Stimulation artifacts



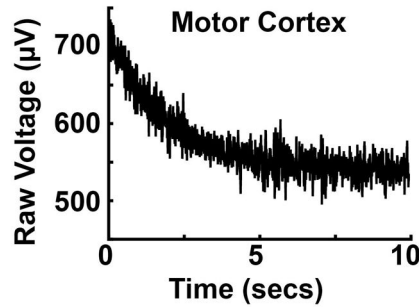
B. Narrowband artifacts



C. EKG artifact



D. Baseline Deflection Artifact



E. Putative Movement Artifacts

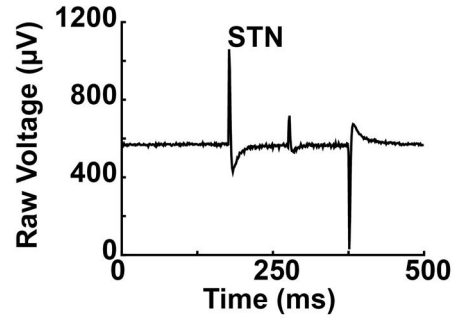


Figure 6. Illustration of common Activa PC+S electrical artifacts. A. Example of DBS stimulation artifacts for constant current and constant voltage settings as well as off DBS in both motor cortex and STN in the same patient (patient 4). Stimulation parameters: c+1–, 160 Hz, 3 V, 60 microseconds pulse-width versus, c+2–, 130 Hz, 4.9 mA, 90 microseconds. Constant voltage recording is at 1 month postoperative, constant current and off stimulation recordings were at 1 year postoperative. Note that in all cases STN recordings were from bipolar contact pairs bordering stimulation to minimize artifact (0–1 for constant voltage recording and 1–3 for constant current and off stimulation). Motor cortex recordings were from contacts 9–11 in all recordings. B. Example of narrowband frequency artifacts

associated with intrinsic firmware properties or clock configuration properties in Active PC +S. See *Results* for more information. C. Example of EKG artifact in STN. D. Example of baseline deflection artifact associated with filter start up transient. This occurred at the beginning of each recording for both electrode contacts. E. Example of transient baseline deflections of unknown etiology. These deflections can occur in motor cortex or STN.

Author Manuscript

Author Manuscript

Author Manuscript

Author Manuscript

Table 1
Patient Characteristics. UPDRS III= Unified Parkinson's Disease Rating Scale – part III, scores.

Patient #	Gender	Age (years)	Disease Duration (years)	Research Hemisphere	Baseline UPDRS Part III (off/on anti-parkinsonian medications)
1	F	47	15	L	68/16
2	M	62	8	R	30/14
3*	F	56	4	L	46/35
4	M	59	7	L	29/14
5	M	60	14	R	44/31

* This patient was subsequently diagnosed with multi-systems atrophy.

Table 2

Patient outcomes. UPDRS III= Unified Parkinson's Disease Rating Scale – part III, scores.

Patient Number	UPDRS III – Baseline off medications	1 year post- operative UPDRS III – off medications, off DBS	1 year post-operative UPDRS III – off medications, on DBS	Percent improvement relative to baseline off medications, at 1 year, off medications, on DBS
1	16 [*]	8 [*]	5 [*]	68% [*]
2	30	22	16	47%
3	46	51	50	9%
4 - unilateral	29	52	41	-41%
5	44	38	22	50%

* Patient tested on medications.

Author Manuscript

Author Manuscript

Author Manuscript

Author Manuscript

ECoG contact and DBS electrode tip coordinates, in mm from the midpoint of the line connecting the anterior and posterior commissures. In each box the top number is the lateral, middle number the anterior-posterior, and lower number the vertical coordinates. The positive direction is defined as right, anterior, and superior.

Table 3

Patient Number	C3	C2	C1	C0	DBS Electrode tip
1	-26.24, -9.61, 63.07	-25.99, -16.79, 64.24	-25.52, -23.35, 64.24	-25.05, -30.15, 64.24	-10.54, -2.73, -4.87
2	30.40, -7.63, 65.36	29.23, -17.86, 66.22	29.23, -27.87, 65.79	29.23, -38.20, 65.47	11.31, -2.35, -4.44
3	-27.52, -4.71, 67.15	-26.35, -15.06, 67.15	-26.74, -25.22, 67.15	-26.94, -35.18, 67.15	-11.39, 0.23, -4.04
4	-38.02, -6.59, 64.21	-38.02, -16.55, 63.63	-38.02, -27.39, 62.75	-38.02, -37.94, 62.46	-12.56, -2.25, -5.96
5	28.43, 5.02, 63.59	28.43, -4.68, 65.94	28.43, -14.90, 67.61	28.43, -25.95, 69.62	12.50, -0.97, -5.51

Table 4

Number of recordings (at rest and on medications) where beta peaks in the LFP or ECoG power spectrum ($>0.25 \log_{10}(\mu\text{V}^2/\text{Hz})$) were detected in STN and motor cortex, by patient.

Patient #	Beta detected - STN (detected/total)	Beta detected – Motor Cortex (detected/total)
1	4/5 (80%)	5/5 (100%)
2	5/5 (100%)	10/10 (100%)
3	2/7 (29%)	14/14 (100%)
4	4/10 (40%)	13/15 (87%)
5	14/15 (93%)	15/18 (83%)
Total	30/42 (71%)	57/62 (92%)

Author Manuscript

Author Manuscript

Author Manuscript

Author Manuscript

Table 5

Number of recordings where movement-related changes in beta and gamma frequencies were detected in STN and motor cortex, by patient.

Patient #	Beta detected - STN (detected/total)	Beta detected – Motor Cortex (detected/total)	Gamma detected - STN (detected/total)	Gamma detected - Motor Cortex (detected/total)
Off DBS				
1	2/5 (40%)	8/9 (89%)	0/5 (0%)	6/9 (67%)
2	11/12 (92%)	12/12 (100%)	5/12 (42%)	12/12 (100%)
3	4/11 (36%)	11/11 (100%)	1/11 (9%)	5/11 (45%)
4	8/11 (72%)	12/12 (100%)	4/11 (36%)	12/12 (100%)
5	9/10 (90%)	11/11 (100%)	3/10 (30%)	2/11 (18%)
Total	34/49 (69%)	54/55 (98%)	13/49 (27%)	37/55 (67%)
On DBS				
1	2/5 (40%)	3/5 (60%)	0/5 (0%)	3/5 (60%)
2	1/9 (0%)	9/9 (100%)	0/9 (0%)	9/9 (100%)
3	1/6 (17%)	6/6 (100%)	0/6 (0%)	1/6 (17%)
4	0/6 (0%)	8/8 (100%)	0/6 (0%)	8/8 (100%)
5	0/0* (0%)	8/8 (100%)	0/0* (N/A%)	4/8 (50%)
Total	4/26 (15%)	34/36 (94%)	0/26 (0%)	25/36 (69%)

* Note: This patient had no STN data during the iPad task on DBS because his DBS utilized 3 contacts (1+2-3-) in order to achieve maximal clinical benefit, leaving no recording contact pairs available.